The Hydration of the Neurotransmitter Acetylcholine in Aqueous Solution

E. C. Hulme,* A. K. Soper,† S. E. McLain,† and J. L. Finney‡

*Division of Physical Biochemistry, MRC National Institute for Medical Research, London, United Kingdom; †ISIS Facility, Rutherford Appleton Laboratory, Chilton, Oxon, United Kingdom; and ‡Department of Physics and Astronomy, University College London, London, United Kingdom

ABSTRACT Neutron diffraction augmented with hydrogen isotope substitution has been used to examine the water structure around the acetylcholine molecular ion in aqueous solution. It is shown that the nearest-neighbor water molecules in the region around the trimethylammonium headgroup are located either in a ring around the central nitrogen atom or between the carbon atoms, forming a sheath around the onium group. Moreover the water molecules in this cavity do not bond to the onium group but rather form hydrogen bonds with water molecules in the surrounding aqueous environment. Given that in the bound state the onium headgroup must be completely desolvated, the absence of bonding between the onium headgroup and the surrounding water solvent may be selectively favorable to acetylcholine-binding in the receptor site. Away from the headgroup, pronounced hydrogen-bonding of water to the carbonyl oxygen is observed, but not to the ether oxygen in the acetylcholine chain.

INTRODUCTION

Acetylcholine (2-(acetyloxy)-*N*,*N*,*N*-trimethylethanaminium (ACh; Fig. 1) was the first identified neurotransmitter. Synthesized by the action of choline acetyltransferase and stored in vesicles in the terminals of cholinergic neurons, it is released into the synaptic cleft by depolarization. Postsynaptically, it acts at two structurally distinct classes of receptors, each having multiple subtypes with unique distributions. They are the nicotinic receptors, which are ligand-gated ion channels that open in a few milliseconds, and the muscarinic receptors (mAChRs), which are G-protein-coupled receptors that initiate intracellular responses in a few tens of milliseconds to several seconds. The neurotransmitter actions of ACh are terminated by extremely rapid hydrolysis by acetylcholinesterase (AChE). The physiological actions of ACh range from muscle contraction and secretion to cognition and memory, and both classes of ACh receptor, as well as AChE, are very important drug targets.

Common themes have emerged from studies of the interactions of acetylcholine and its analogs with both receptors and hydrolase. The first is the key role of aromatic side chains in binding the positively-charged headgroup (1). The crystal structure of the complex between carbamylcholine (CCh) and molluscan ACh binding proteins (a model for the ACh binding site of nicotinic receptors) shows the onium headgroup to be enclosed in a box of tryptophan and tyrosine residues (2). Exhaustive mutagenesis studies have predicted that a charge-stabilized aromatic cage surrounds the headgroup of ACh bound to the M_1 mAChR (3–5). Aromatic residues guide ligands through the entrance gorge of AChE into the catalytic site where a tryptophan residue is the key to onium binding (6).

The second is desolvation of the ligand and displacement of water molecules from the binding site. In AChBP, water molecules are visible in the open conformation of the binding site of the apoprotein but are largely or completely excluded by an inward movement of contact residues on binding the ligand (2,7). Closure of the aromatic cage around the onium headgroup of ACh may help to trigger the activation of the M_1 mAChR (8); a suggestion that has also received experimental support (9). In AChE, water molecules, poorly ordered in the apoprotein, are excluded from the onium binding surface by bound ligands (10).

In each case, the development of the interactions made in the bound state requires desolvation of the onium group. Conversely, the nature of the water cage around the onium headgroup in solution must influence the energetics of binding. The structure of water around the tetramethylammonium ion, which has the same structure as the ACh headgroup, has been studied by neutron diffraction with isotopic substitution, where both the onium and water hydrogen sites have been labeled. This ion has been shown to conform to an apolar rather than an ionic mode of hydration (11–13). Here we report the extension of the technique to study the hydration structure around the headgroup of the ACh molecule itself. The results also show the hydration of the ester group, which is thought to participate in a hydrogen-bonding network in the mAChR binding site (3,14), and is the subject of nucleophilic attack in AChE.

In this instance, a well-proven technique using isotopic labeling allowed for the direct determination of the solvent-solvent, solvent-solute, and solute-solute correlations in various solutions (15,16). Explicitly, the isotopic substitution was used for the water solvent itself and then on both the headgroup and water simultaneously to probe a maximum number of correlations. The first set of substitutions yields the water-water correlations, whereas the second set gives a combination of water-water, ACh-water, and ACh-ACh correlations. Additionally, the experimental data have been modeled using the disordered materials program empirical

Submitted May 15, 2006, and accepted for publication June 13, 2006.

Address reprint requests to S. E. McLain, ISIS Facility, Rutherford Appleton Laboratory, Chilton, Didcot, Oxon OX11 0QX, UK. E-mail: s.mclain@rl.ac.uk.

0006-3495/06/09/2371/10 $2.00

doi: 10.1529/biophysj.106.089185

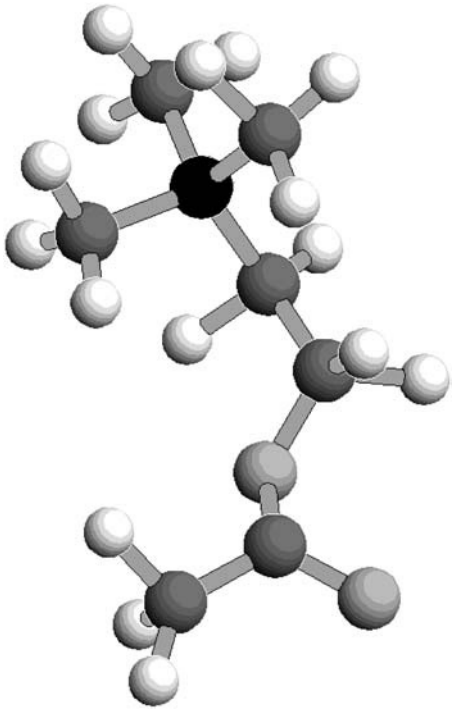

FIGURE 1 Molecular structure of acetylcholine, where the light gray atoms are oxygen, the dark gray atoms are carbon, the white atoms are hydrogen, and the black atom is nitrogen.

potential structure refinement (EPSR) (17,18). Although there have been a few neutron diffraction studies of biological molecules in aqueous solution (19–21), (S. E. McLain, A. K. Soper, and A. Watts, unpublished data), this report is among the first applications applying both experimental and computational techniques to the molecular-level structural study of these molecules in an aqueous environment.

THEORETICAL OVERVIEW

Neutron diffraction with isotopic substitution is an excellent technique to study the structure of hydrogen-containing fluids, mixtures of fluids, and solutions (12,13,15,16,19,21–31). This is due to the difference in scattering intensity by hydrogen and deuterium, which have scattering intensities of $b_H = -3.73$ fm and $b_D = 6.671$ fm, respectively. This difference allows for the measurement of chemically identical, yet isotopically distinct, samples from which several different diffraction patterns can be measured for a given system.

In a multicomponent system where some or all of the hydrogen atoms present can be isotopically substituted, the diffraction pattern obtained by neutron scattering can be described by the total structure factor, $F(Q)$, which is a sum of three composite partial structure factors (CPSF), $H_{\alpha\beta}(Q)$, each weighted by their respective concentrations in the sample and their neutron scattering intensities. This allows $F(Q)$ to be written as

$$F(Q) = c_X^2 b_X^2 H_{XX}(Q) + 2c_X c_Y b_X b_Y H_{XY}(Q) + c_Y^2 b_Y^2 H_{YY}(Q), \quad (1)$$

where $Q = (4\pi \sin\theta)/\lambda)$ is the wave vector of scattered neutrons at the scattering angle 2θ and λ is the neutron wavelength. X refers to the atoms that have not been isotopically substituted, and Y refers only to the substituted atoms (hydrogen in this case). The atomic fraction, c_X and c_Y, and the corresponding scattering lengths, b_X and b_Y, are weighted sums over the values for the individual atoms that appear in the CPSFs, namely,

$$c_X = \sum_{\alpha \neq Y} c_\alpha,\ c_Y = \sum_{\alpha = Y} c_\alpha,\ b_x = \sum_{\alpha \neq Y} c_\alpha b_\alpha / c_X,\ \textit{and}$$
$$b_Y = \sum_{\alpha = Y} c_\alpha b_\alpha / c_Y. \quad (2)$$

Therefore, it follows that each individual CPSF, $H_{XX}(Q)$, $H_{XY}(Q)$, and $H_{YY}(Q)$ can be written as a sum over individual atom-atom partial structure factors (32). For example,

$$H_{XX}(Q) = \frac{1}{c_X^2 b_X^2} \sum_{\alpha \neq Y} \sum_{\beta \neq Y} c_\alpha c_\beta b_\alpha b_\beta H_{\alpha\beta}(Q), \quad (3)$$

with equivalent expressions for the other terms.

For acetylcholine in aqueous solution we have distinguished between the hydrogen atoms on the onium headgroup (M) and the hydrogen on the water molecules (H_w), so in an experiment where both types of hydrogen are substituted the $H_{YY}(Q)$ correlation contains contributions from three terms, namely, $H_{HwHw}(Q)$, $H_{HwM}(Q)$, and $H_{MM}(Q)$. Of these, the $H_{HwHw}(Q)$ function is derived solely from the water hydrogen-hydrogen correlations. On the other hand $H_{HwM}(Q)$ is a direct measure of the correlation between methyl hydrogens on the onium headgroup and water hydrogens, whereas $H_{MM}(Q)$ yields the onium methyl-methyl hydrogen correlations. Compared to these $H_{YY}(Q)$ terms, the $H_{XX}(Q)$ and $H_{XY}(Q)$ terms are more complex to interpret as they contain many intra- as well as intermolecular correlations on and between the acetylcholine and water molecules.

The Fourier transform of any structure factor yields the associated radial distribution function which, analogous to the CPSFs, is the sum of the respective atom-atom radial distribution functions (RDFs) $g_{\alpha\beta}(r)$s, each weighted by concentration and scattering length of atomic species (α and β) present in the sample analogous to Eq. 1. The CPSFs are related to the RDFs via the Fourier transform,

$$H_{\alpha\beta}(Q) = 1 + \frac{4\pi\rho}{Q} \int r[g_{\alpha\beta}(r) - 1]\sin(Qr)dr. \quad (4)$$

The RDFs show the distances in one-dimensional real space on an Ångstrom length scale between atoms present in the solution. Additionally, integration of $g_{\alpha\beta}(r)$ gives the coordination number of atoms β around α atoms between two distances, r_1 and r_2 as

$$n_{\alpha}^{\beta}(r) = 4\pi\, c_{\beta}\rho \int_{r1}^{r2} g_{\alpha\beta}(r) r^2 dr, \quad (5)$$

where ρ corresponds to the atomic number density of the sample and c_β is the concentration of atom β. The coordination number is usually taken by integration up to the first minimum (r_{min}) after the first obvious peak in the RDF.

To extract each of the RDFs from the measured data, as well as to provide insight into the average structure of the system in three dimensions, computer refinement procedures are employed. The EPSR technique was used to model the extracted CPSFs from the neutron diffraction measurements and hence allow the determination of the partial RDFs of the system. EPSR, a computational method for modeling disordered materials such as liquids and glasses (17,31), allows for three-dimensional information to be extracted from a set of one-dimensional structure-factor measurements in a manner that is consistent with the measured data. The procedure begins with a standard Monte Carlo simulation using an initial reference potential consisting of an intramolecular harmonic potential to define the geometry of the molecules being modeled, and an intermolecular potential, which, here, consists of Lennard-Jones 12-6 potentials for the site-site interactions on different molecules, as well as Coloumbic interactions for some sites. This initial reference potential is used to generate a starting configuration of molecules in a simulation box at the appropriate density of the system. EPSR then iteratively adjusts a perturbation to this reference potential to obtain agreement between the simulated $H_{\alpha\beta}(Q)$ and the experimental diffraction data (17,31), thus providing for the extraction of three-dimensional structural information that is consistent with the measured data.

Any structure factor can be expanded into a series of spherical harmonic coefficients that can be used to determine the location of atoms or molecules relative to one another as well as the orientational distribution of these molecules with respect to the others (32). For example, in this study spherical harmonic expansion was performed to determine the orientation of water molecules about the onium headgroup (vide infra). Details of the spherical harmonic expansion, as well as the orientational correlation function calculation, are given in detail elsewhere (16,32); however, for completeness, a summary of these techniques is presented here.

A set of Euler angles within the laboratory reference frame $\omega_M \equiv (\varphi_M \theta_M \chi_M)$ for each molecule M is calculated using a predefined set of molecular coordinate axes. The corresponding set of generalized spherical harmonic functions, $D^{l}_{mn}(\omega_M)$, are calculated for each molecule and for a range of (l,m,n) values (up to $l = 6$ in this instance). The set of such functions is then correlated, taking into account the relative position $\mathbf{r} \equiv (r, \omega_L) \equiv (r, \phi_L, \theta_L)$ of the second molecule with respect to the first, yielding a set of orientational correlation function expansion coefficients, $g(l_1 l_2 l; n_1 n_2; r)$. From these coefficients, the full orientational pair correlation function is obtained as an expansion of the form:

$$g(\mathbf{r}, \omega_1, \omega_2) = \sum_{l_1 l_2 l} \sum_{m_1 m_2 m} \sum_{n_1 n_2} g(l_1 l_2 l; n_1 n_2; r) \times C(l_1 l_2 l; m_1 m_2 m) D^{l_1}_{m_1 n_1}(\omega_1)^* D^{l_2}_{m_2 n_2}(\omega_2)^* D^{l}_{m0}(\omega_1), \quad (6)$$

where $C(l_1 l_2 l; m_1 m_2 m)$ are the Clebsch-Gordan coefficients, ω_1 represents the Euler angles of molecule 1, ω_2 represents the Euler angles of molecule 2, and $\mathbf{r} = (r, \omega_L)$ represents the position of molecule 2 relative to molecule 1 in the laboratory coordinate frame.

To reconstruct the orientational correlation function, it is convenient to set molecule 1 at the origin and orient it so that $\omega_1 = 0$. This serves to define the coordinate system about which the spatial density and orientation of second (neighboring) molecules will be plotted. It also leads to an immediate simplification of Eq. 6 in that $D^{l}_{mn}(000) = \delta(mn)$, so that combining this with the requirement from the Clebsch-Gordan coefficients that $m = m_1 + m_2$, the orientational pair correlation function relative to a central molecule at the origin is given by

$$g(r, \omega, \omega_M) = \sum_{l_1 l_2 l} \sum_{m} \sum_{n_1 n_2} g(l_1 l_2 l; n_1 n_2; r) C(l_1 l_2 l; n_1 m_2 m) D^{l_2}_{m_2 n_2}(\omega_M)^* D^{l}_{m0}(\omega_L), \quad (7)$$

where $m_2 = m - n_1$. The spatial density function is generated by averaging the full orientational pair correlation function over the orientations of the second molecule, $\omega_M \equiv (\varphi_M \theta_M \chi_M)$, which immediately eliminates any terms in the summation shown in Eq. 6 for which $l_2, m_2, n_2 \neq 0$. Hence the spatial density function is expressed as

$$g(r, \omega) = \sum_{l_1} \sum_{n_1} g(l_1 0 l_1; n_1 0; r) C(l_1 0 l_1; n_1 0 n_1) D^{l_1}_{n_1 0}(\omega_L), \quad (8)$$

from the closure relations for the Clebsch-Gordan coefficients ($l_1 + l_2 \geq l \geq |l_1 - l_2|$).

In general, the full orientational pair correlation function (Eq. 6) is difficult to visualize because it is a function of six coordinates. To assist in this visualization, the spatial density function can be plotted to gauge the most likely places of finding neighboring molecules; then the orientational correlation function can plotted for a specified ω_L, after either fixing or averaging over one of the remaining angular coordinates. This eliminates from some of the terms from Eq. 6, leaving an average orientational pair correlation function which is a function of three variables.

EXPERIMENTAL

Acetylcholine (*N*,*N*,*N*-trimethyl-d_9) bromide (99% D) was purchased from MSD Isotopes (Montreal, Canada) and fully protiated acetylcholine bromide was purchased from Sigma Chemical (Poole, Dorset, UK) and recrystallized from dry acetone before use. Both fully deuterated and fully protiated acetylcholine bromide samples were dried to constant weight in a drying pistol before the addition of D_2O and

H_2O, respectively, to give a mole fraction of 1 acetylcholine bromide per 50 water molecules (~1 M). The other solutions, described below, were prepared from these deuterated and protiated stock solutions. The integrity of each solution was checked by NMR spectroscopy after the neutron diffraction experiment and there was no evidence of hydrolysis in any of the samples.

Neutron diffraction measurements were taken on aqueous solutions of the bromide salt of acetylcholine (ACh) and in each case the molar concentration was slightly less than 1 M: specifically, each sample contained 1 molecule AChBr per 50 water molecules. This concentration was chosen because it allows for a significant signal to be observed for the AChBr molecules in solution while minimizing solute-solute interactions, thus insuring the full hydration of the ACh cation. For each measurement, the samples were contained in flat plate cells constructed from Ti/Zr alloy where in each case the sample thickness was 1 mm. The use of this alloy is advantageous, as the coherent signal from the container itself is minimal. Additionally, Ti/Zr is largely resistant to corrosion by ionic molecules in aqueous systems. Diffraction data were recorded for ~12 h, at ambient temperature, for each sample on the SANDALS diffractometer located at the ISIS pulsed neutron source in the United Kingdom. Corrections to the data for background effects, as well as normalization, were performed using standard analysis procedures (33): the procedures for extraction of the CPSFs ($H_{\alpha\beta}(Q)$) has been described in detail elsewhere (15).

A total of seven isotopomeric samples of 1:50 AChBr/water were measured. These were d_9-AChBr in H_2O, D_2O and HDO (50:50 H_2O/D_2O); h-AChBr in H_2O and D_2O; and 50:50 d_9-AChBr/h-AChBr in HDO and D_2O. As mentioned above, labeling the water hydrogens H_w, the onium methyl hydrogens M, and all other atoms—including the water oxygens, the remaining atoms of the ACh molecules, and the bromine ions—X, combinations of the diffraction data collected from these solutions yielded three sets of partial structure factors: 1), H_w/H_w, $H_w/M + X$, $X + M/X + M$; 2), $M + H_w/M + H_w$, $M + H_w/X$, X/X; and 3), M/M, $M/X + H_w$, $X + H/X + H_w$. However, due to beam failure at the end of the experiment the last data set (3) was measured at another time under different experimental conditions. Additionally, the signal from the samples for data set 3 was weak due to the low concentration of atoms with a significant scattering intensity, so that information from this data set was unreliable and was therefore discarded.

The EPSR modeling box was constructed using 20 AChBr molecules and 1000 water molecules to give a molecular ratio of 1:50 AChBr/water molecules at an atomic density of 0.1 atoms/$Å^{-3}$. The starting reference potentials are listed for each atom in Table 1. In this table, O_w and H_w refer to the water oxygen and hydrogen atoms, respectively and the starting reference potentials for these atoms were taken from the SPC/E potentials (34). From this table, with reference to Fig. 1, O_1 is the ether oxygen, O_2 the C=O (carbonyl) oxygen, H the hydrogen atoms on the backbone of the ACh molecule, C_1 the onium methyl carbons, M the onium methyl hydrogens, and C_2 the backbone carbons. The initial reference potentials for these atoms were adapted from the SPC/E potentials for water, with the charges adjusted to achieve electroneutrality in the system. Specifically, the ACh molecule has an overall net charge of +1, whereas the bromine has an overall charge of −1, and the water molecules are neutral.

TABLE 1 EPSR reference potentials for fits to the neutron diffraction data

Atom	ε/kJ · mol^{-1}	σ/Å	q_e
O_w	0.65	3.166	−0.8476
H_w	0.0	0.0	0.4238
Br	0.2704	5.05	−1.00
O_1	0.648	3.166	−0.5
O_2	0.648	3.166	−0.5
H	0.2	1.70	0.0
C_1	0.606	3.96	0.333
N	0.650	3.25	0.0
M	0.2	1.7	0.0
C_2	0.606	3.96	0.25

RESULTS AND DISCUSSION

The CPSFs extracted from diffraction data taken for the acetylcholine water solution are shown along with the subsequent EPSR fits to these CPSFs in Fig. 2. It can be seen from this figure that the model fits to the data are good, with the exception of the low Q region (~0–2 $Å^{-1}$), where inelasticity and background effects are the most difficult to remove in samples containing light hydrogen.

The H_wH_w CPSF (Fig. 2) allows for the examination of the H_wH_w correlation between water molecules in the solution and is shown in Fig. 3. Also shown in Fig. 3 are the RDFs for

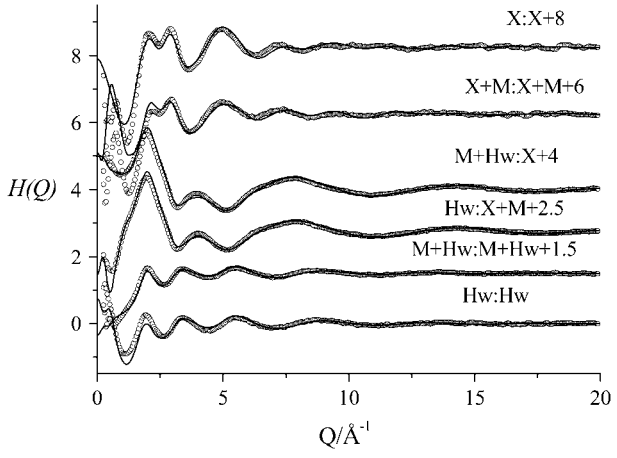

FIGURE 2 Measured composite structure factors (*circles*) and EPSR fits (*solid lines*) for AChBr in water. *M*, methyl hydrogens; *Hw*, water hydrogens; *X*, all other atoms present in the system.

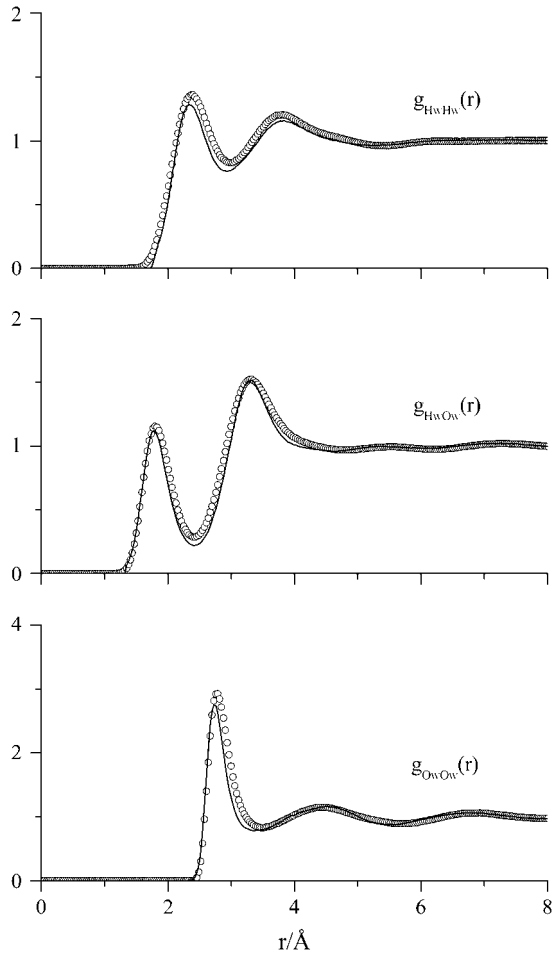

FIGURE 3 Water-water RDFs from AChBr in solution (*circles*) compared with the case of pure water (*lines*).

the other water correlations ($g_{OwHw}(r)$ and $g_{OwOw}(r)$) extracted from the EPSR model. Each of the functions shown is compared with the equivalent curve for pure water (31). The water-water RDFs from the present solution show a marked similarity to the corresponding curve for pure water. This indicates that the structure of the bulk water solvent is predominantly preserved upon the addition of AChBr. The peaks in each of the RDFs are in the same positions and there is only a slight difference in peak shape between AChBr/water and pure water. The absence of a significant difference indicates that the ACh molecule can be incorporated into the water structure with no major modifications to the local water structure, thereby leaving the average tetrahedral bulk water network mostly intact. The fact that there is no large difference between the water RDFs in pure water and in the AChBr/water solution can be understood to arise from the fact that the bulk water solvent essentially forms a hole that incorporates the molecules in the solution without significantly changing the bulk water structure.

Fig. 4 shows the RDFs relating to the water onium interactions. The M-water correlations are quite broad, which is to be expected given that the bulk water structure remains intact. On the other hand, both the onium methyl carbons and the nitrogen atom show quite strong interactions with the surrounding water as both $g_{C1Ow}(r)$ and $g_{NOw}(r)$ have quite strong peaks at 3.4 Å and 4.8 Å, respectively, with the $g_{NOw}(r)$ function showing an additional shoulder before the peak at 4.8 Å. These strong correlations are also reproduced in the $g_{C1Hw}(r)$ function, which shows two peaks, one at ~4 Å and the other at ~5.8 Å, whereas the $g_{NHw}(r)$ function shows one strong peak at ~4.8 Å. This indicates that although the water molecules have a broader distribution of interactions with the onium methyl hydrogens, they form quite strong interactions with the carbons from the methyl group and the central nitrogen atom. It would appear that water molecules surround the heavier atoms of this group (N and C) while having a very limited interaction with the M hydrogen sites. This view is consistent with the M-water correlations, which show a strong intensity (Fig. 4) at larger values of r (~4.2 Å and 6.2 Å in the $g_{MOw}(r)$ function and ~6.3 Å in the $g_{MHw}(r)$ function). This is also consistent with the bulk water network being largely unperturbed as the water oxygen atoms show the strongest interactions and the hydrogen atoms are likely pointed away from the onium headgroup and are therefore available for hydrogen bonding to the bulk water network. Inspection of the $g_{NOw}(r)$ coordination number at $r_{min} = 6.0$ Å shows that there are 23 water molecules surrounding the nitrogen atom in the onium group. This is similar to what was found in an independent study of the tetramethylammonium ion in aqueous solution (11–13).

The RDFs associated with the two oxygen sites from ACh with water are shown in Fig. 5. Again, from Fig. 1 and Table 1, O_1 is the ether oxygen and O_2 is the carbonyl oxygen from the ester group. From this figure, it is clear that the carbonyl oxygen has the strongest correlation with the water environment, whereas the ether oxygen interactions with water are quite broad, though both of these atoms possess the same fractional charge in the simulation. The coordination numbers for the two O_2 RDFs shown in Fig. 5 are $n_{O_2}^{Hw} = 1.9$ at $r_{min} = 2.55$ Å and $n_{O_2}^{Ow} = 2.2$ at $r_{min} = 3.36$ Å. These results suggest that two different water molecules hydrogen-bond to the carbonyl oxygen, indicating that the hydrogen-bonding capacity of the carbonyl oxygen is saturated. This tentative conclusion is confirmed by the orientational information discussed below.

The spatial density functions (SDFs) from the EPSR fits to the data have been extracted as described above for the water distributions around the onium group, as well as the water distribution around the C=O group (vide infra). To generate these functions for the ACh onium headgroup, shown on the central axes in Fig. 6, *a* and *b*, the nitrogen atom is set at the origin and the geometric midpoint of the three methyl carbon atoms is used to define the z axis. One of these carbon atoms is then used to define the zx plane. From these axes, it is possible to probe the distribution of water molecules

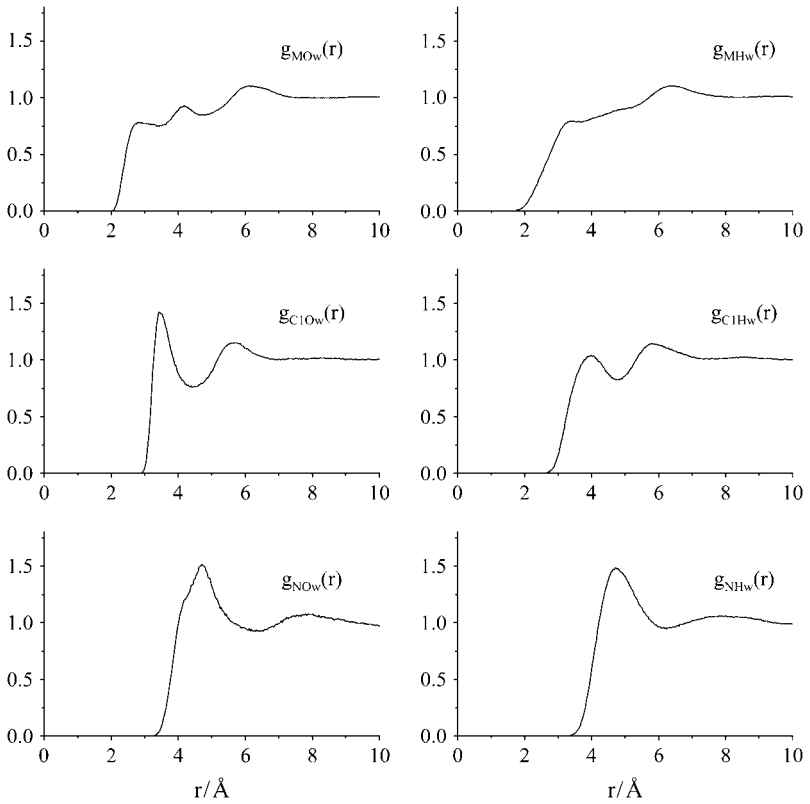

FIGURE 4 RDFs for the onium-water interactions extracted from the EPSR fits to the diffraction data.

surrounding this group. Fig. 6, *a* and *b*, shows the location of water molecules as a shell around the onium headgroup in respective ranges of 0– 4.5 Å and 4.5–6 Å. These distance values were chosen from the $g_{NOw}(r)$ function (Fig. 4). The first distance range corresponds to the area of the shoulder in the $g_{NOw}(r)$ function, namely from the origin to the first peak maximum at ~4.5 Å corresponding roughly to a first coordination shell. The second distance range is from the peak maxium to the first minimum at ~6 Å, corresponding roughly to a second coordination shell. In these figures, the surface contour level has been set so that 80% of the molecules present are depicted in the surrounding solvent shell for Fig. 6 *a* and 20% of the molecules are depicted in Fig. 6 *b*.

From Fig. 6 *a*, the most likely location of water molecules occupying the nearest-neighbor shell around the onium headgroup are distributed in a band around the central nitrogen atom or in ''strips'' between the carbon groups above the *xz* plane and also directly above the headgroup. There is a clear absence of water molecules directly in front of the carbon atom and below the headgroup. The presence of density in the first coordination shell between the methyl groups shows that the water molecules fill the ''clefts'' between these groups; this result is consistent with studies on tertiary-butyl alcohol, where the same phenomenon was observed (27). In Fig. 6 *b*, which corresponds to the next nearest-neighbor shell, the water molecules are located in a shell in front of the carbon atoms and above the *z* axis, with an absence of distribution below the onium headgroup. The absence of density below in Fig. 6, *a* and *b*, is as expected, as this is the space occupied by tail of the ACh molecule.

To determine the orientation of the molecules in the surrounding shell, the orientational correlation functions (OCFs), described above, were extracted at two separate locations corresponding to the distribution shown in Fig. 6. Specifically, Fig. 7 *a* shows the OCF of water molecules from $r =$ 2–4.5 Å surrounding the onium ion at $\omega_L = (\phi_L, \theta_L) =$ (0, 100) relative to the onium headgroup corresponding to the band of density around the central nitrogen atom shown in Fig. 6 *a*. In this figure, a representative water molecule is shown on the central axis with the shell showing the orientational probability distribution of the water molecule's dipole moment vector as a function of ϕ_M and θ_M, with the central water pointing toward the most likely orientation. At this location, it is clear that the water dipole is approximately tangential to the group, but points slightly away from the headgroup on average. This orientation of the water molecules relative to the onium group enables the water molecules at this location to form hydrogen bonds between other water molecules in the solvent, but there are no bonds to the onium group itself.

Fig. 7 *b*, on the other hand, shows the orientation of water molecules from $r = 0$–4.5 Å directly above the *z* axis in Fig. 6, at $\omega_L = (\phi_L, \theta_L) = (0, 0)$ relative to the onium headgroup. Here the dipole moment vector is plotted as a function of ϕ_M and χ_M to depict the orientation of the dipole relative

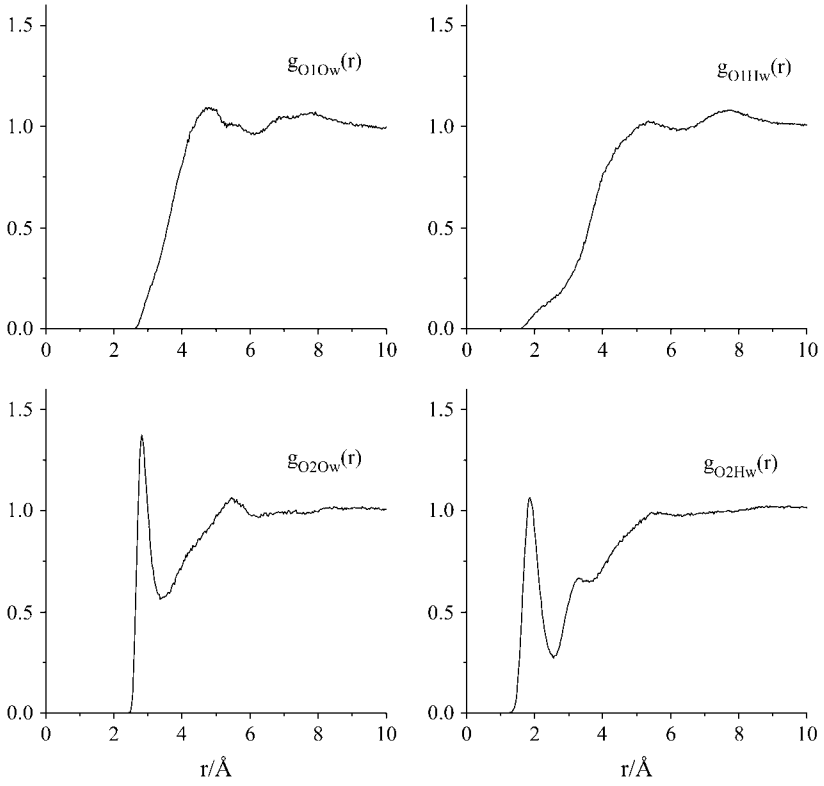

FIGURE 5 RDFs for the ester oxygen (O1)-water correlations and the carbonyl oxygen (O2)-water correlations extracted from the EPSR fits to the diffraction data.

to the central onium group. Similar to Fig. 7 *a*, it is clear that the dipole orientation of the water molecules is also roughly tangential to the onium headgroup, as was the case with tetramethylammonium in aqueous solution (11), but with a tendency to point slightly away from the ion on average.

It is clear from Fig. 7 that the preferred direction of the water orientation about the onium headgroup is with the molecules arranged so as to maximize their interaction with the bulk water solvent rather than with the onium headgroup. Fig. 8 shows a diagrammatic representation of the orientation of water molecules from Fig. 7, *a* and *b*, relative to the central onium headgroup of the ACh molecule. In this figure, the negative portion of the water dipole is indicated by δ^-. Taken together, Figs. 7 and 8 indicate that the water molecule dipole is tangential to the headgroup on average, though directly above the onium group the water dipole has a radial component, indicating that the inside surface of the water cavity is negatively charged.

Fig. 9 shows the SDFs for the carbonyl group on ACh. In this case, the oxygen atom was set at the origin of the coordinate axes with the C=O bond defining the *z* axis; additionally, the *zx* plane is defined by the ether oxygen (not shown). This figure shows 75% of the molecules surrounding the C=O group from $r = 0$–3.5 Å. It can be seen that there is no density directly below the carbonyl group (*z* axis).

Fig. 10 shows the orientation of the water molecules surrounding the carbonyl group in a similar fashion to that of Fig. 7 *a*, where the orientations of the surrounding molecules

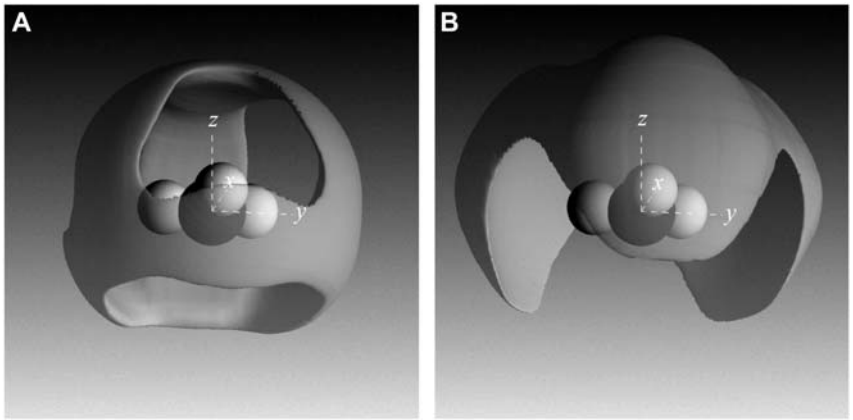

FIGURE 6 Spatial density functions (SDFs) for water molecules surrounding the onium headgroup (on the central axis) from ACh extracted from the EPSR fits to the diffraction data. (*a*) SDF from 2 to 4.5 Å, where the contour level of the surrounding shell encompasses 80% of the molecules. (*b*) SDF from 4.5 to 6 Å, where the contour levels of the surrounding shell encompass 25% of the surrounding water molecules. In each case, the dimension of the plotting box is 12 Å, where the atom at the origin of the axis is the nitrogen and the surrounding white atoms represent the onium carbons. The methyl hydrogens have been eliminated for clarity.

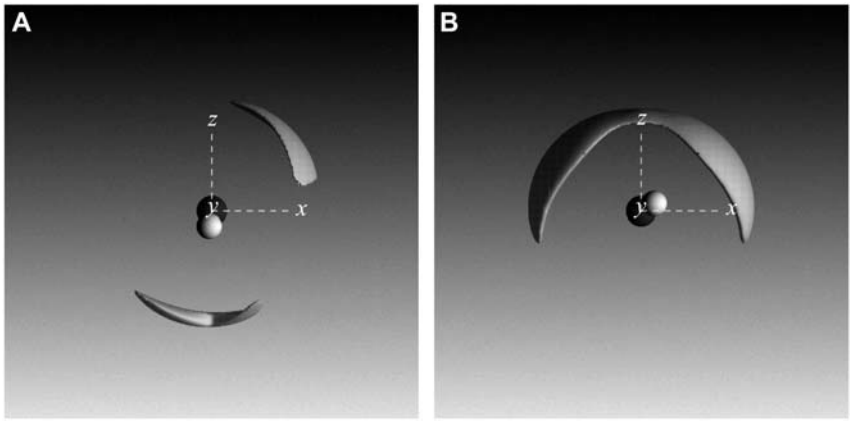

FIGURE 7 Orientational correlation functions (OCFs) for water molecules in the first shell surrounding the onium headgroup in the ACh molecule extracted from the EPSR fits to the diffraction data. (*a*) OCF from 2 to 4.5 Å at a position of $\phi_L = 0$, θ_L=100 relative to the central onium headgroup shown in Fig. 6. (*b*) OCF at the same distances above the onium headgroup at $\phi_L = 0°$, $\theta_L = 0°$ relative to the central molecule. In each case, a representative water molecule is placed on the central axis and is oriented toward the most likely orientation and the dimension of each plotting box is 12 Å. The contour level of the orientational shell is set to encompass 35% of the molecules in *a* and 50% in *b*, and the water molecule in each panel is pointed toward the most likely orientation. Additionally, both figures have been rotated by 90° for clarity.

are assessed as a function of ϕ_M and θ_M at a position of $\omega_L = (\phi_L, \theta_L) = (0, 30)$ relative to the central carbonyl group over a range of r = 0–3.5 Å. The surrounding shell again shows the most probable orientation of water molecules in this region, where the water molecule itself is orientated toward the highest probability location. The orientation of the water molecule around the C=O group is with one of the hydrogen atoms pointed toward the carbonyl oxygen, indicating hydrogen bonding from the water molecule. This confirms the tentative conclusion drawn earlier from the partial RDFs concerning the likely hydrogen-bonding of water to the carbonyl oxygen.

CONCLUSIONS

ACh is a molecule that simultaneously displays polar and apolar properties, though it is a charged ion. The bulk water structure is not disrupted by the incorporation of the acetylcholine molecule at the concentrations studied; the large headgroup can apparently be incorporated into solution without a significant perturbation to the water structure itself, where the charge on the nitrogen atom has been shielded from the surrounding water environment by delocalization onto methyl ligands. The water molecules surrounding the onium group on ACh show no strong hydrogen bonding interactions with the methyl groups or with the onium nitrogen. Along the chain of the molecule, the only atom that hydrogen-bonds with the surrounding water solvent is the carbonyl oxygen, where approximately one hydrogen bond is provided by one water molecule for an average of two hydrogen bonds to the carbonyl oxygen from two different water molecules saturating the carbonyl oxygen's hydrogen-bonding capability. The hydrogen bonding here does not significantly affect the bulk water structure but is rather easily incorporated into the surrounding water solvent. In contrast, the ether oxygen, despite its polar nature, shows an absence of direct interaction with the surrounding waters.

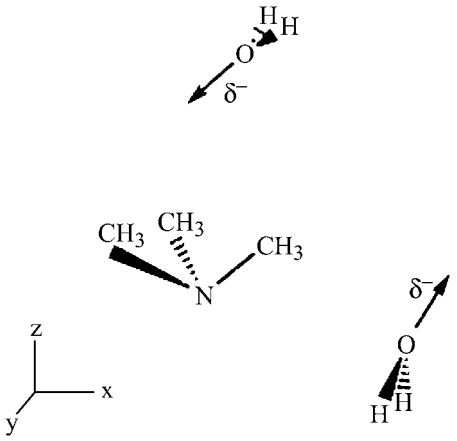

FIGURE 8 Representation of water molecule orientation surrounding the onium headgroup.

FIGURE 9 SDF for water molecules surrounding the carbonyl group from ACh extracted from the EPSR fits to the diffraction data from 0 to 3.5 Å, where the contour levels of the surrounding shell encompass 70% of the surrounding water molecules. The dimension of the plotting box is 12 Å and the oxygen atom (*white*) is located at the origin of the axes, whereas the carbon (*black*) is directly below, defining the –*z* axis.

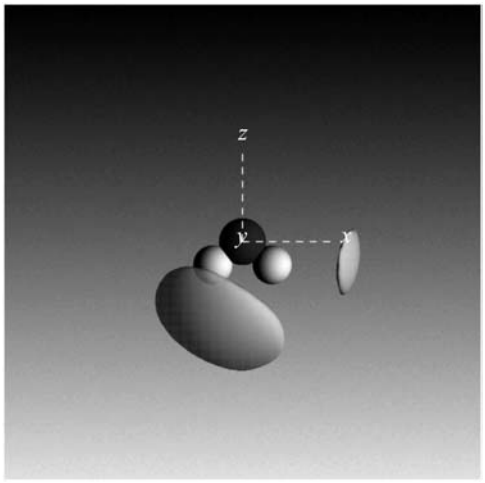

FIGURE 10 Water OCF at a position of $\phi_L = 0$, $\theta_L = 30$ relative to the carbonyl group on the central axis in the first nearest-neighbor shell (1–3.5 Å) surrounding the carbonyl oxygen extracted from the EPSR fits to the diffraction data. Here the dimension of the plotting box is 12 Å, the contour level is set to encompass 80% of the water molecules, and the water molecule is oriented to show the most likely orientation.

The implications of these results for understanding the binding energetics of ACh to a receptor protein are significant. Given that in the bound state the onium headgroup must be partly or completely desolvated, the absence of strong directional bonding between the onium headgroup and the surrounding water solvent may be selectively favorable to acetylcholine binding in the receptor site. The structural similarities of bulk water and the water surrounding the headgroup suggest that any entropic contribution to the binding of the onium headgroup is unlikely to arise from an increase in disorder upon the return of the water in the first nearest-neighbor shell back to the bulk water environment. This is consistent with other results on the hydration of nonpolar groups (11,12,16), which also implies that the entropic contribution to hydrophobic interactions is unlikely to come from release of ordered water as implied by the classical model of Frank and Quist (35). The origin of the entropic contribution to the hydrophobic interactions thus remains a matter of debate, perhaps relating to the entropic costs of creating a ''hole'' in the solvent large enough to accommodate the ACh molecule (36).

In contrast, recent studies have emphasized the role of enthalpic forces in driving ligand binding. Favorable enthalpy changes arising from desolvation of the interface between the ligand and its binding partner have been designated the nonclassical hydrophobic effect (37), and these may well be more relevant to the binding of ACh, through cation-π interactions (38–40).

Water molecules are visible in the x-ray structure of the open conformation of apo-AChBP (7), but are excluded when the CCh-AChBP complex forms (2), particularly from the aromatic box that encloses the onium headgroup. Although there is no such direct structural evidence in the mAChRs, the similar amino acid composition of the aromatic cage (3–5) and the inward movement that has been deduced to accompany receptor activation (8,9) suggest that in this protein desolvation may accompany the binding of the ACh headgroup. An interesting analysis of buried water molecules in x-ray structures of AChE and its ligand complexes (10) has shown that water molecules associated with hydrophobic subsites in the active-site aromatic gorge of the enzyme are poorly ordered, probably forming weak interactions with the π-electrons of the side chains. These ''activated'' waters are suboptimally H-bonded by ~0.8 H-bonds per molecule. As a result, they are loosely packed, leaving voids, and are readily displaced by incoming ligands.

Water molecules with unsatisfied H-bonding potential in aromatic onium binding pockets, if they are indeed a general phenomenon, may be regarded as the mirror image of water molecules around the headgroup of ACh revealed in the present study. The displacement of these ''unsatisfied'' waters into the cavity vacated by the incoming ligand would provide a component of the binding energy. This would primarily be an enthalpic effect, summating with the dispersion forces of the ligand-receptor interaction itself. Indeed, the binding of ACh and CCh to AChBP, and of CCh to brain and heart mAChRs has been reported to be driven primarily by enthalpy rather than entropy changes (2,41,42).

Does the hydrogen-bonding pattern of the ACh ester group also have implications for receptor binding? In the AChBP complex, the ester group of carbachol does not seem to be involved in specific hydrogen bonds (2), although no structure is available for the complex with bound ACh. In the mAChRs, it has been proposed that the ester group of ACh hydrogen-bonds to the hydroxyl groups of tyrosine residues in the aromatic cage (3–5) or participates in a hydrogen-bonding network incorporating tyrosine and threonine OH groups (14). Whether or not the water molecules hydrogen-bonded to the ester carbonyl group are stripped away or retained as part of a network should have implications for the energetics of ACh binding, but this issue cannot be settled without a high-resolution crystal structure of the complex. Interestingly, classical structure-activity studies showed that the ethoxy-ethyl derivative of ACh, in which the ether oxygen alone is preserved, has higher muscarinic potency and efficacy than the keto derivative, in which the ether oxygen is replaced by a methylene group (43).

S. E. McLain acknowledges the financial support of the United States National Science Foundation (OISE-0404938).

REFERENCES

1. Zacharias, N., and D. A. Dougherty. 2002. Cation-π interactions in ligand recognition and catalysis. *Trends Pharmacol. Sci.* 23:281–287.
2. Celie, P. H., S. E. Rossum-Fikkert, W. J. Van Dijk, K. Brejc, A. B. Smit, and T. K. Sixma. 2004. Nicotine and carbamylcholine binding to nicotinic acetylcholine receptors as studied in AChBP crystal structures. *Neuron.* 41:907–914.

3. Lu, Z. L., J. W. Saldanha, and E. C. Hulme. 2001. Transmembrane domains 4 and 7 of the M-1 muscarinic acetylcholine receptor are critical for ligand binding and the receptor activation switch. *J. Biol. Chem.* 276:34098–34104.
4. Hulme, E. C., Z. L. Lu, and M. S. Bee. 2003. Scanning mutagenesis studies of the M-1 muscarinic acetylcholine receptor. *Receptors Channels.* 9:215–228.
5. Hulme, E. C., Z. L. Lu, J. W. Saldanha, and M. S. Bee. 2003. Structure and activation of muscarinic acetylcholine receptors. *Biochem. Soc. Trans.* 31:29–34.
6. Harel, M., I. Schalk, L. Ehret-Sabatier, F. Bouet, M. Goeldner, C. Hirth, P. H. Axelsen, I. Silman, and J. L. Sussman. 1993. Quaternary ligand binding to aromatic residues in the active-site gorge of acetylcholinesterase. *Proc. Natl. Acad. Sci. USA.* 98:9031–9035.
7. Hansen, S. B. 2005. Structures of Aplysia AChBP complexes with nicotinic agonists and antagonists reveal distinctive binding interfaces and conformations. *EMBO J.* 24:3635–3646.
8. Lu, Z. L., J. W. Saldanha, and E. C. Hulme. 2002. Seven-transmembrane receptors: crystals clarify. *Trends Pharmacol. Sci.* 23:140–146.
9. Han, S. J., F. F. Hamdan, S. K. Kim, K. A. Jacobson, L. M. Bloodworth, B. Li, and J. Wess. 2005. Identification of an agonist-induced conformational change occurring adjacent to the ligand-binding pocket of the M(3) muscarinic acetylcholine receptor. *J. Biol. Chem.* 280:34849–34858.
10. Koellner, G., G. Kryger, C. B. Millard, I. Silman, J. L. Sussman, and T. Steiner. 2000. Active-site gorge and buried water molecules in crystal structure of acetycholinesterase from *Torpedo californica*. *J. Mol. Biol.* 296:713–735.
11. Turner, J. Z., A. K. Soper, and J. L. Finney. 1995. Ionic versus apolar behavior of the tetramethylammonium ion in water. *J. Chem. Phys.* 102:5438–5443.
12. Turner, J. Z., A. K. Soper, and J. L. Finney. 1990. A neutron diffraction study of tetramethylammonium chloride in aqueous solution. *Mol. Phys.* 70:679–700.
13. Turner, J. Z., A. K. Soper, and J. L. Finney. 1992. Water structure in aqueous solutions of tetramethyl ammonium chloride. *Mol. Phys.* 77: 411–429.
14. Furukawa, H., T. Hamada, M. K. Hayashi, T. Haga, Y. Muto, H. Hirota, S. Yokoyama, K. Nagasawa, and M. Ishiguro. 2002. Conformation of ligands bound to the muscarinic acetylcholine receptor. *Mol. Pharmacol.* 62:778–787.
15. Soper, A. K., and A. Luzar. 1992. A neutron-diffraction study of dimethyl sulfoxide-water mixtures. *J. Chem. Phys.* 97:1320–1331.
16. Soper, A. K., and J. L. Finney. 1993. Hydration of methanol in aqueous solution. *Phys. Rev. Lett.* 71:4346–4349.
17. Soper, A. K. 2001. Tests of the empirical potential structure refinement method and a new method of application to neutron diffraction data on water. *Mol. Phys.* 99:1503–1516.
18. Soper, A. K. 2005. Partial structure factors from disordered materials diffraction data: an approach using empirical potential structure refinement. *Phys. Rev. B.* 72:104204.
19. Kameda, Y., K. Sugawara, T. Usuki, and O. Uemura. 2003. Hydration structure of alanine molecule in concentrated aqueous solutions. *Bull. Chem. Soc. Jpn.* 76:935–943.
20. Branca, C., V. Magazu, G. Maisano, F. Migliardo, and A. K. Soper. 2002. Study on destructuring effect of trehalose on water by neutron diffraction. *Appl. Phys. A.* 74:S450–S451.
21. Soper, A. K., E. W. Castner, and A. Luzar. 2003. Impact of urea on water structure: a clue to its properties as a denaturant? *Biophys. Chem.* 105:649–666.
22. Reference deleted in press.
23. McLain, S. E., C. J. Benmore, J. E. Siewenie, J. Urquidi, and J. F. C. Turner. 2004. On the liquid structure of hydrogen fluoride. *Angew. Chem. Int. Ed. Engl.* 43:1952–1955.
24. Botti, A., F. Bruni, S. Imberti, M. A. Ricci, and A. K. Soper. 2004. Ions in water: the microscopic structure of concentrated NaOH solutions. *J. Chem. Phys.* 120:10154–10162.
25. Botti, A., F. Bruni, S. Imberti, M. A. Ricci, and A. K. Soper. 2005. Solvation shell of OH^- ions in water. *J. Mol. Liq.* 117:81–84.
26 Bowron, D. T. and J. L. Finney. 2002. Anion bridges drive salting out of a simple amphiphile from aqueous solution. *Phys. Rev. Lett.* 89: 215508.
27. Bowron, D. T., J. L. Finney, and A. K. Soper. 1998. Structural investigation of solute-solute interactions in aqueous solutions of tertiary butanol. *J. Phys. Chem. B.* 102:3551–3563.
28. Soper, A. K., and R. N. Silver. 1982. Hydrogen-hydrogen pair correlation function in liquid water. *Phys. Rev. Lett.* 49:471–474.
29. Thompson, H., J. C. Wasse, N. T. Skipper, S. Hayama, D. T. Bowron, and A. K. Soper. 2003. Structural studies of ammonia and metallic lithium-ammonia solutions. *J. Am. Chem. Soc.* 125:2572–2581.
30. Turner, J. F. C., and A. K. Soper. 2004. On the determination of the structure of ferrocene in solution. *Polyhedron.* 23:2975–2983.
31. Soper, A. K. 2000. The radial distribution functions of water and ice from 220 to 673 K and at pressures up to 400 MPa. *Chem. Phys.* 258:121–137.
32. Gray, C. G., and K. E. Gubbins. 1984. Theory of Molecular Liquids. Vol I: Fundamentals. Oxford University Press, New York.
33. Soper, A. K., W. S. Howells, and A. C. Hannon. 1989. ATLAS. Analysis of Time-of-Flight Diffraction Data from Liquid and Amorphous Samples. RAL report number RAL-89.046. Rutherford Appleton Laboratory, Oxon, UK.
34. Berendsen, H. J. C., J. R. Grigera, and T. P. Straatsma. 1987. The missing term in effective pair potentials. *J. Phys. Chem.* 91:6269–6271.
35. Frank, H. S., and A. S. Quist. 1961. Pauling's model and the thermodynamic properties of water. *J. Chem. Phys.* 34:604–611.
36. Lee, B. 1994. Enthalpy-entropy compensation in the thermodynamics of hydrophobicity. *Biophys. Chem.* 51:271–278.
37. Meyers, E. A., R. K. Castellano, and F. Diederich. 2003. Interactions with aromatic rings in chemical and biological recognition. *Angew. Chem. Int. Ed. Engl.* 42:1210–1250.
38. Watts, A. 2005. Solid state NMR in drug design and discovery for membrane embedded targets. *Nature Reviews Drug Discovery.* 4:555–568.
39. Williamson, P. T. F., G. Grobner, P. J. R. Spooner, K. W. Miller, and A. Watts. 1998. Probing the agonist binding pocket on the nicotine acetylcholine receptor: a high resolution solid state NMR approach. *Biochemistry.* 37:10854–10859.
40. Williamson, P. T. F., J. A. Watts, G. H. Addona, K. W. Miller, and A. Watts. 2001. Dynamics and orientation of N+(CD3)3- bromoacetylcholine to its binding site on the nicotinic acetylcholine receptor. *PNAS.* 98:2346–2351.
41. Waelbroeck, M., P. Robberecht, P. Chatelain, P. Deneef, and J. Christophe. 1985. Effects of temperature and ethanol on agonist and antagonist binding to rat-heart muscarinic receptors in the absence and presence of GTP. *Biochem. J.* 231:469–476.
42. Gies, J. P., B. Ilien, and Y. Landry. 1986. Muscarinic acetylcholine receptor: thermodynamic analysis of the interaction of agonists and antagonists. *Biochim. Biophys. Acta.* 889:103–115.
43. Ing, H. R., P. Kordik, and D. P. H. Tudor-Williams. 1952. Studies on the structure-action relationships of the choline group. *Br. J. Pharmacol. Chemother.* 7:103–116.